

This version of the ESI replaced the original version on 18th August 2022 due to the original missing Figure S1 on page 3.

Electronic Supplementary Information:

One-Step Synthesis of Nanocrystalline Transition Metal Oxide on Thin Sheets of Disordered Graphitic Carbon by Oxidation of MXenes

Michael Naguib,^{a,b} Olha Mashtalir,^{a,b} Maria R. Lukatskaya,^{a,b} Boris Dyatkin,^{a,b}
Chuanfang Zhang,^{a,b} Volker Presser,^c Yury Gogotsi^{a,b} and Michel W. Barsoum^{*b}

^a *Department of Materials Science & Engineering, Drexel University, Philadelphia, PA 19104, USA*

^b *A. J. Drexel Nanomaterials Institute, Drexel University, Philadelphia, PA 19104, USA.*

^c *INM – Leibniz Institute for New Materials & Saarland University, 66123 Saarbrücken, Germany*

I. Materials Characterization

To investigate the phase and structural changes occurring as a result of the oxidation, X-ray diffraction, XRD, patterns were collected using a diffractometer (Rigaku, SmartLab, Tokyo, Japan) with Cu-K α radiation (step scan 0.02° 2 θ , 1 s per step). Silicon, Si, powder was added to some samples as an internal standard to calibrate the diffraction angles and instrumental peak broadening. A Raman spectrometer (Renishaw inVia, Peltier-cooled CCD array detector, Gloucestershire, United Kingdom) was also used to characterize the oxidized powders. An argon, Ar, ion laser radiation (514.5 nm) was focused to a spot size of ~ 2 μ m using a power of less than 1 mW.

The morphological changes occurring upon oxidation were investigated using a scanning electron microscope, SEM, (Zeiss, Supra 50VP, Oberkochen, Germany) and a transmission electron microscope, TEM, (JEOL JEM-2100, Akishima, Japan) using an accelerating voltage of 200 kV. Specimens for TEM analysis were prepared by suspending powders in isopropanol, sonicating for 5 min, and placing a drop on a 200 mesh lacey-carbon-coated copper grids (LC200-Cu, Electron Microscopy Sciences, Hatfield, PA, USA). The elemental compositions were determined using an energy dispersive X-ray (EDX) analyzer, AMETEK/EDAX Genesis attachment (EDAX Inc., Mahwah, NJ, USA), mounted on the TEM.

To investigate the changes in surface area, gas sorption analysis was carried out (Autosorb-1, Quantachrome Instruments, Boynton Beach, FL, USA) using nitrogen, N₂, and Ar adsorbates, at -196 °C. Prior to the analysis, the samples were outgassed under vacuum at 120 °C for 48 h. The adsorption isotherms of the different gases at -196 °C were analyzed and used to calculate the specific surface area (SSA) using the Brunauer-Emmet-Teller (BET) equation. P/P₀ values between 0.05 and 0.10 were used to calculate the SSA via multi-point BET.

II. Li-ion Batteries (LIBs) Coin Cell Preparation and Testing

Electrodes of the oxidized MXene powders were prepared by mixing them with 10 wt.% carbon black, and 10 wt. % polyvinylidene fluoride, PVDF, dissolved in 1-methyl-2-pyrrolidinone. The mixture was spread on a Cu foil using a doctor blade and dried at 140 °C for 12 h under a mechanical vacuum (<1.3 kPa). The electrodes' loading was about 3 mg·cm⁻². A stainless steel coin cell (type CR-2016, MTI, Richmond, CA, USA) configuration was used to test the electrochemical performance. Lithium, Li, metal foils were used as counter electrodes. Borosilicate glass fibers (Whatman GF/A) were used as separators. The electrolyte used was 1 M lithium hexafluorophosphate (LiPF₆) solution in a 1:1 by mass mixture of ethylene carbonate and diethyl carbonate (EC:DEC).

The coin cells were assembled in an Ar filled glove box, with nominally less than 1 ppm of O₂ or H₂O. Galvanostatic charge-discharge cycling was carried out using a battery cycler (Arbin BT-2143- 11U, College Station, TX, USA) to find the capacity and study the cyclabilities at different rates. For cyclic voltammetry (CV) testing, a potentiostat (VMP3, Biologic, Knoxville, TN, USA) was used. Electrochemical testing was performed between 0.0 – 3.0 V vs. Li/Li⁺.

III. Oxidized Delaminated MXene

In brief, $\text{Ti}_3\text{C}_2\text{T}_x$ was soaked in dimethyl sulfoxide (DMSO) for 18 h at room temperature, centrifuged at 3500 rpm, before sonicating the DMSO intercalated powders in water for 6 h, which resulted in a suspension of d- $\text{Ti}_3\text{C}_2\text{T}_x$ in water. The suspension was then centrifuged to separate the sediment from the supernatant (colloidal solution of d- $\text{Ti}_3\text{C}_2\text{T}_x$ in water) that was in turn used to fabricate freestanding MXene paper by filtration. **Figure S1A** shows XRD patterns for delaminated MXene paper before and after flash oxidation in air at 1150 °C for 30 s.

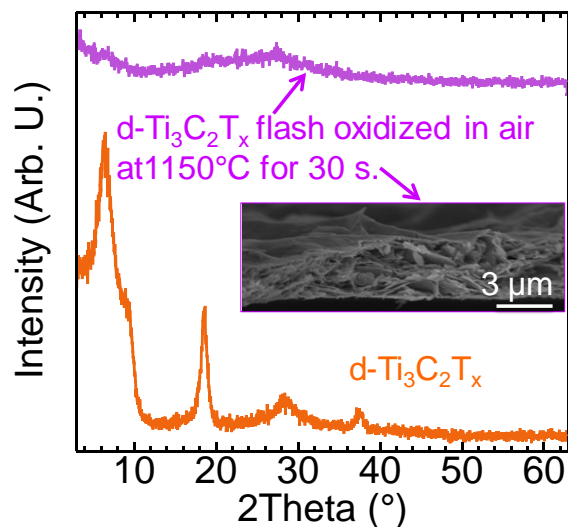


Fig. S1 XRD patterns of delaminated $\text{Ti}_3\text{C}_2\text{T}_x$ paper before and after flash oxidation the inset shows a cross-sectional SEM image for d-MXene paper after flash oxidation at 1150 °C for 30 s in air.

IV. Isothermal Oxidation in CO_2

Powders of $\text{Ti}_3\text{C}_2\text{T}_x$ were exposed to a continuous flow of carbon dioxide, CO_2 , at 150, 300, and 500 °C. The procedure was the following: 200 mg of $\text{Ti}_3\text{C}_2\text{T}_x$ powders were loaded into a horizontal quartz tube furnace. The tube was purged with Ar for 30 min, followed by heating in continuous Ar flow, at a rate of 10 °C·min⁻¹, to the desired temperature. Once the desired temperature was established, the Ar gas was replaced by CO_2 . The flow rate was 10 sccm. After holding during 1 h at the required temperature, the sample was cooled to room temperature in an Ar environment.

Figure S2A shows the XRD patterns of $Ti_3C_2T_x$ before and after CO_2 treatment at different temperatures. At 150 °C, $Ti_3C_2T_x$ was the main phase with small amounts of anatase. After the 300 °C treatment, significant amounts of anatase co-exist with $Ti_3C_2T_x$. After the 500 °C treatment, the fraction of not oxidized $Ti_3C_2T_x$ was greatly reduced.

A typical SEM image of CO_2 treated $Ti_3C_2T_x$ sample in **Figure S2B** shows small uniform oxide particles residing within the layers with a few, relatively large, cuboids of oxide at the edge of the layers. The presence of both anatase and amorphous carbon after the 300 °C oxidation was confirmed by Raman spectroscopy (**Figure S2C**).

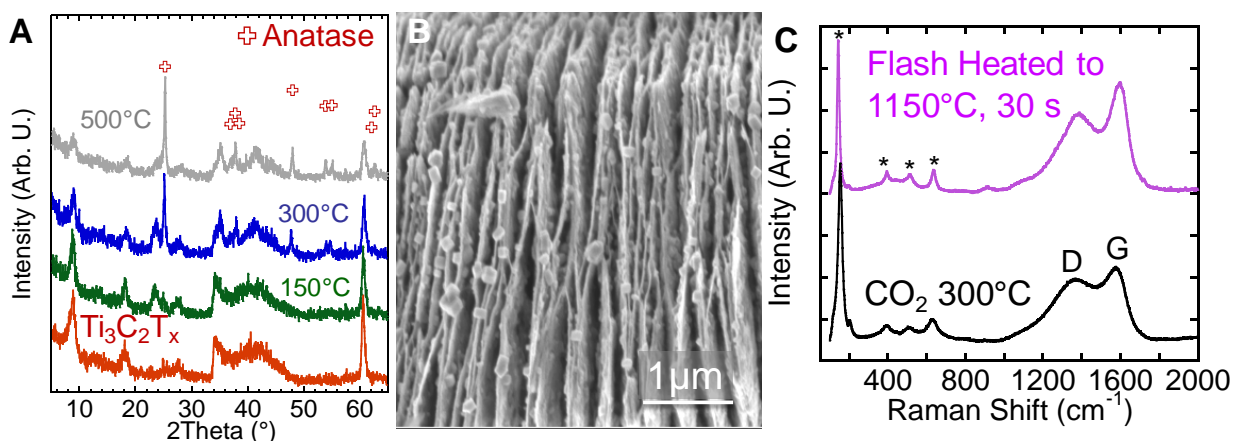


Fig. S2 (A) XRD patterns of $Ti_3C_2T_x$ powders before and after CO_2 oxidation. Red crosses represent locations of anatase peaks, (B) SEM image of a $Ti_3C_2T_x$ particle after CO_2 oxidation at 300 °C for 1 h; (C) Raman spectra for $Ti_3C_2T_x$ after CO_2 oxidation at 300 °C for 1 h and flash oxidation in air at 1150 °C for 30 s, the * signs represent the anatase peaks positions, while the D and G represent the D- and G-bands of carbon.

V. Hydrothermal Oxidation

A stainless steel autoclave fitted with a 300 mL Teflon chamber was used for hydrothermal treatment of $Ti_3C_2T_x$ in deionized (DI) water. The following conditions were used: 150 °C for 48 h; 200 °C for 8, 12, and 20 h; and 250 °C for 2 h. The heating rate from room temperature to the treatment temperatures was 5 °C/min. The estimated pressure inside the autoclave was about 1, 2, and 5 MPa at 150, 200, and 250 °C, respectively. In all the cases 1 g of $Ti_3C_2T_x$ powder was

dispersed in 100 mL of DI water. After treatment, the suspensions were centrifuged at 3000 rpm to separate the particles from the water.

XRD patterns, for all hydrothermally treated samples (**Figure S3**), show peaks for both anatase and MXene. With increasing holding time at a certain temperature, the intensities of the anatase peaks grow at the expense of the MXene peak intensities. This reflects the kinetics of the oxidation process as a carbide consuming mechanism. In all the cases, complete coverage with the nanoparticles was observed using SEM. **Figure S4** shows the SEM images for samples treated at 150 °C for 48 h and at 250 °C for 2 h.

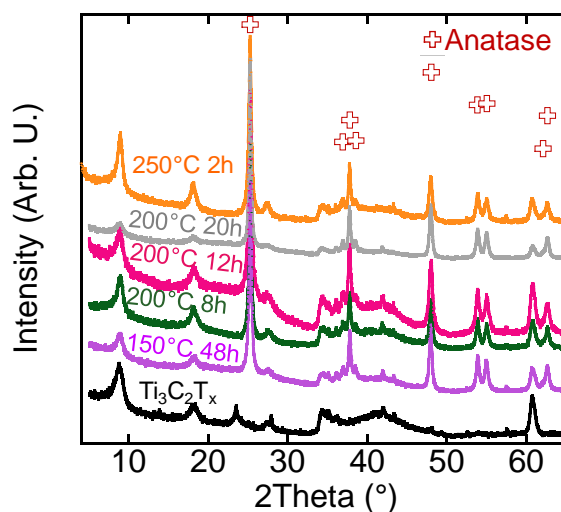


Fig. S3 XRD patterns of $\text{Ti}_3\text{C}_2\text{T}_x$ before and after hydrothermal treatment at different temperatures and time intervals. The red crosses represent anatase.

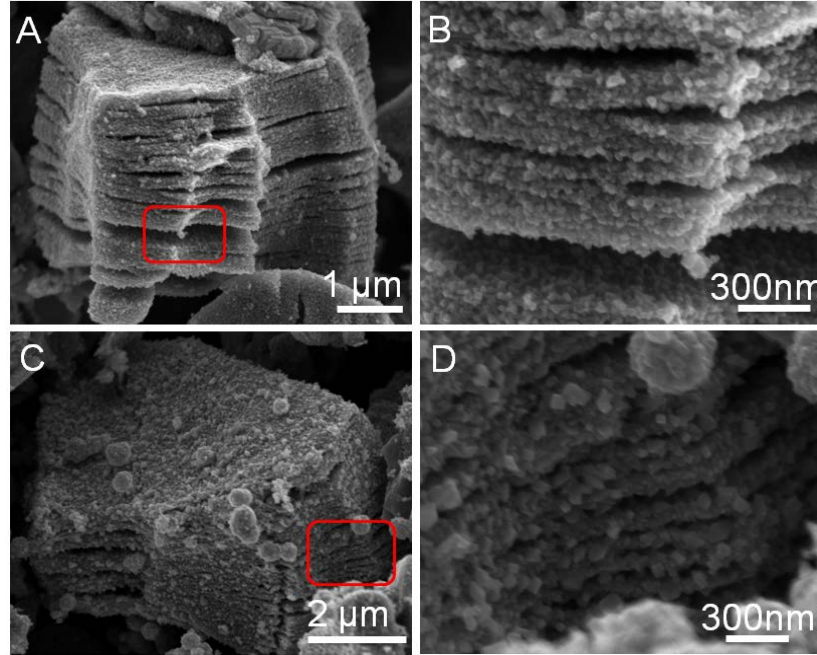


Fig. S4. SEM images of $\text{Ti}_3\text{C}_2\text{T}_x$ after hydrothermal treatment in DI water at: A) 150 °C for 48 h, and B) zoom in on the region framed in (A), C) 250 °C 2h, D) zoom in on the region framed in (C).

Figure S5 shows the cyclic voltammograms for a MXene sample that was hydrothermally treated sample at 250 °C for 2 h, and used as an electrode material in LIBs, compared to those for the flash oxidized sample. Both samples showed similar features for nanocrystalline anatase, viz. lithiation and delithiation peaks around 1.7 V and 2.2 V, respectively, vs. Li/Li^+ . The delithiation peak for the hydrothermally treated sample was shifted to a lower voltage as compared to the flash oxidized sample (2.1 V instead of 2.2 V). A larger area inside the CVs can be observed for the sample that was prepared by flash oxidation (solid lines in **Figure S5**) compared to that for the sample prepared hydrothermally (dashed lines in **Figure S5**). This means that more energy is stored in the case of flash oxidation. The reason for this observation is unknown at this time, but is a topic of continued research.

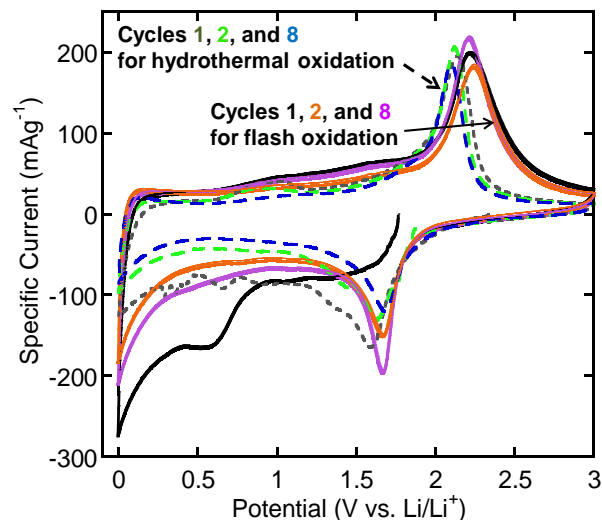


Fig. S5. Cyclic voltammograms for oxidized $\text{Ti}_3\text{C}_2\text{T}_x$ produced by flash oxidation (solid curves) and hydrothermal oxidation (dashed curves). Cycled at $0.2 \text{ mV}\cdot\text{s}^{-1}$.

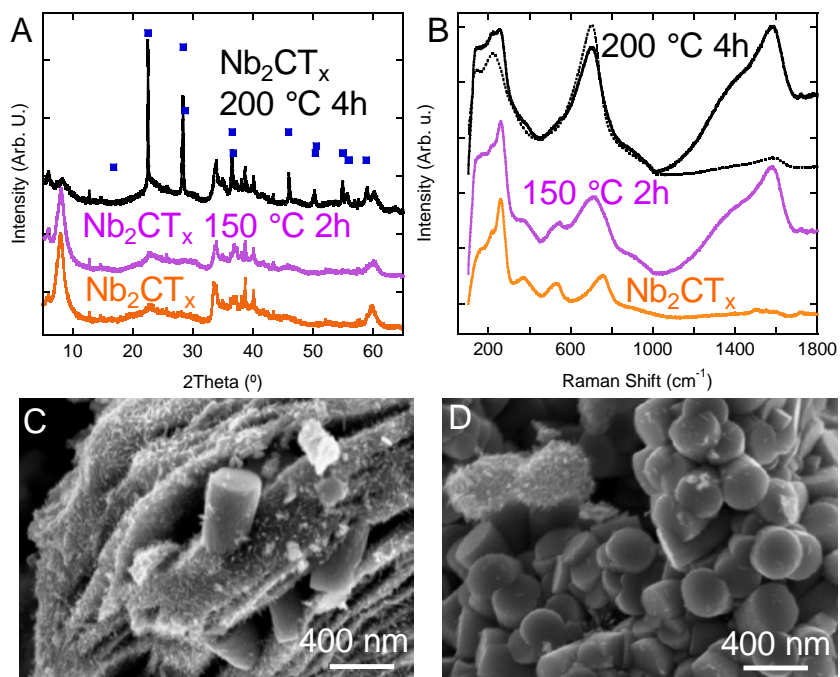


Fig. S6 A) XRD patterns and B) Raman spectra for Nb_2CT_x before and after hydrothermal treatment at $150 \text{ }^\circ\text{C}$ for 2 h and $200 \text{ }^\circ\text{C}$ for 4 h. The blue squares in (A) represent peaks position of Nb_2O_5 (PDF#27-1312); black dotted line in (B) represents Raman spectrum at a different location in the same sample that was treated at $200 \text{ }^\circ\text{C}$ for 4 h where carbon was *not* observed. SEM images of Nb_2CT_x samples after hydrothermal treatment at, C) $150 \text{ }^\circ\text{C}$ for 2 h and, D) $200 \text{ }^\circ\text{C}$ for 4 h.